ACS APPLIED POLYMER MATERIALS

pubs.acs.org/acsapm Article

# Visible Light-Triggered Microactuators and Dynamic Surfaces from Hydrogels Containing Photoswitchable Host−Guest Complexes

Joseph C. Roback, Montana B. Minnis, Kesete Ghebreyessus,* and Ryan C. Hayward*

Cite This: https://doi.org/10.1021/acsapm.4c00917 Read Online



**ABSTRACT:** Light-responsive hydrogels garner considerable interest due to their ability to undergo a wide variety of shape transformations that can be triggered remotely and with fine spatiotemporal control. To this end, photoswitchable supramolecular complexes offer a convenient route to tune hydrophilicity of hydrogels; however, thus far, this approach has required the use of potentially damaging ultraviolet light. To address this limitation, we introduce a light-responsive supramolecular hydrogel that can be addressed entirely with visible light using a hydrogel with pendant thiomethyl-substituted arylazopyrazole (SMe-AAP) in a solution of beta-cyclodextrin ($\beta$-CD). Upon irradiation with purple light, *trans*−*cis* isomerization triggers a swelling response in the hydrogels that is rapid, stable, and reversible under green light. Remarkably, this result suggests stronger binding of $\beta$-CD to the cis isomer, which is opposite to the behavior for most reported azo photoswitches. To shed further insights into this behavior, we characterize the binding between SMe-AAP and $\beta$-CD using calorimetry and 2D-NOESY NMR spectroscopy. Finally, we demonstrate that the SMe-AAP hydrogels can be used to fabricate functional materials, including micron-scale bending actuators and surface wrinkles with precisely patterned morphologies.

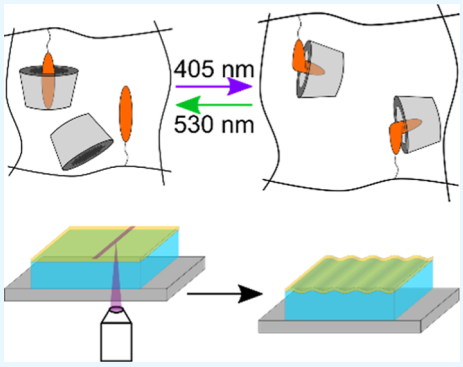


**KEYWORDS:** *responsive hydrogels, host−guest complex, actuators, surface wrinkles*

## ■ INTRODUCTION

Stimuli-responsive hydrogels can offer a diverse range of capabilities such as shape-morphing,[1,2] actuation,[3,4] and locomotion[5,6] and can function in biomedical applications such as drug delivery and cell culture.[7−11] Generally, the applied stimulus triggers a swelling or deswelling response of the hydrated polymer network, and although there exist many possible stimuli to address responsive hydrogels, light is particularly attractive due to its remote delivery and the high degree of spatiotemporal control it affords. A significant amount of literature has leveraged photothermal effects in temperature-sensitive hydrogels to drive volume change, an approach which typically exhibits large response magnitude and operates under visible light.[12−16] However, photothermally addressable materials require constant illumination to maintain a volume change and suffer from decreased patterning resolution due to thermal broadening.[17]

Alternatively, incorporation of photochemical moieties such as spiropyran into hydrogels can generate significant volume change upon irradiation with blue light due to the large change in hydrophilicity between the ring-open merocyanine and ring-closed spiropyran isomers.[18−20] However, the need to protonate the merocyanine isomer in an acidic environment to generate swelling limits their use in biological applications where materials must operate in narrow pH ranges,[21] and the spiropyran isomer spontaneously ring-opens in 10s of minutes in aqueous solutions, thus limiting the stability.[22] Further approaches involve the use of photodissociable molecules or[23,24] photoinduced dimerization[25] or leveraging photoredox chemistry.[26] While these strategies can result in large volume changes in response to irradiation and can be operated with visible light, they are limited by rapid reversion kinetics or harsh shape-reprogramming conditions.

Azobenzene and related photoswitches are widely used in photoresponsive materials due to attractive properties including highly tunable lifetimes and excellent photostability;[27] however, swelling in azobenzene-containing hydrogels is driven by the modest change in polarity between *cis* and *trans* isomers, which typically limits the magnitude of light response.[28] To enhance this effect, our group has previously studied photochemically driven shape changes in hydrogels using host−guest interactions between azobenzene and $\alpha$-cyclodextrin ($\alpha$-CD).[29] Cyclodextrins (CDs) are macrocyclic oligosaccharides that have a toroidal shape with a hydrophilic exterior and a hydrophobic inner cavity, allowing them to

Received: March 25, 2024
Revised: May 15, 2024
Accepted: May 16, 2024

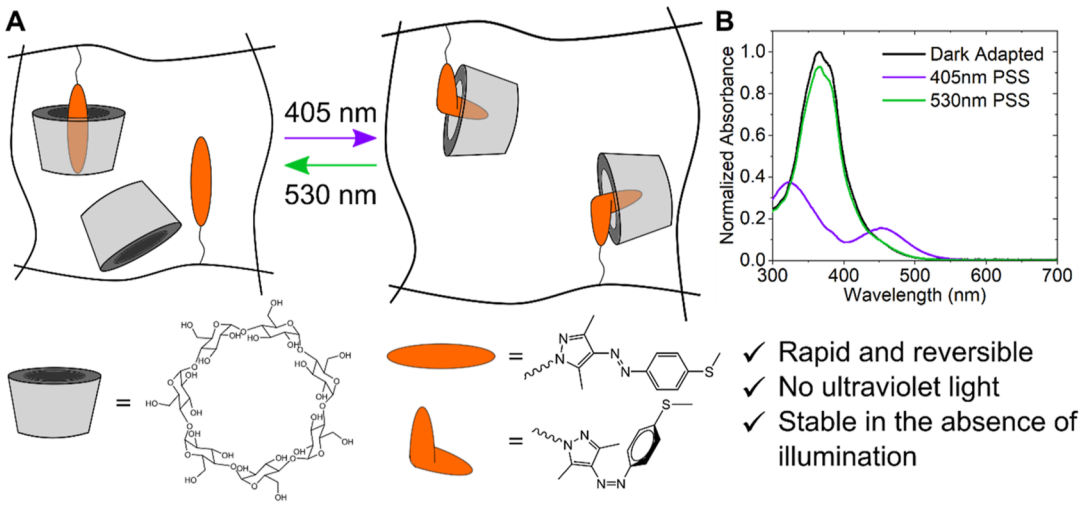


**Figure 1.** (A) Chemical structure and schematic showing hydrogels with SMe-AAP pendant groups that swell upon *trans*−*cis* isomerization. (B) UV−vis spectra of SMe-AAP-Ac (0.025 mg/mL in DMSO) after equilibration in the dark (black line), after irradiation with 405 nm light (purple line), and after irradiation with 530 nm light (green line).

encapsulate appropriately sized hydrophobic molecules.[30] When an azobenzene monomer in the *trans* configuration is incorporated into a hydrogel network and immersed in a solution of $\alpha$-CD, a host−guest complex is formed, increasing the hydrophilicity of the network and driving swelling. However, when the azobenzene is isomerized to the *cis* configuration using ultraviolet (UV) light, the molecule is no longer compatible with the CD cavity, and the complex is destroyed, resulting in shrinking of the network. Photoreversible complexation between azobenzene and CDs has also been widely employed to trigger sol−gel transitions, to alter network mechanical properties through tuning of cross-link density,[31−33] and to drive actuation using slide-ring-based designs in both hydrated and dry materials.[34,35] While these approaches have the benefit of rapid, reversible, and stable shape change, the need for UV light limits light penetration into the material and may lead to issues in future biomaterials applications due to the potential for large doses of UV light to inflict cellular damage.

Several other azobenzene derivatives have also been reported to form photoreversible complexes with CDs and can offer other attractive properties such as red-shifted absorption spectra, higher conversion at the photostationary state (PSS), and greater thermal stability of the *cis* isomer.[36−40] These properties can allow for greater penetration depth of light, improved compatibility with materials for cell and tissue culture, and more persistent shape changes. In this work, we specifically focus on a methyl thioether-substituted arylazopyrazole (SMe-AAP), first reported by Bhunia, Dolai, and Samata.[41] This molecule was chosen for a number of interesting photophysical properties including high photoconversion using visible light (96% *cis* reported at the 400 nm PSS and 96% *trans* reported at the 530 nm PSS) and a high thermal half-life of the *cis* isomer (2.8 d). Additionally, while the method of preparation of the SMe-AAP has been described in the literature, its potential applications particularly with regard to host−guest chemistry have not yet been explored. We demonstrate that hydrogels containing SMe-AAP undergo rapid and reversible light-triggered swelling upon *trans*−*cis* isomerization in a solution of $\beta$-CD (Figure 1A), a result opposite to that of our previously reported supramolecular hydrogels using azobenzene and $\alpha$-CD. We then characterize the binding behavior between the SMe-AAP and $\beta$-CD to elucidate the swelling mechanism. Finally, we show that these hydrogels can be used for the fabrication of light-responsive trilayer microactuators and as a method to program patterned surface wrinkles into bilayer hydrogels. Due to their operation exclusively under visible light (Figures 1B and S2, S3), these materials open the door for functional devices with improved biocompatibility.

## RESULTS AND DISCUSSION

To characterize the light-induced swelling response of the AAP-containing host−guest hydrogel, we first prepared thin sheets of hydrogels by free radical polymerization of *N*-isopropylacrylamide (NIPAM), *N*,*N*′-methylenebis-(acrylamide) (BIS), and an acrylate-functionalized thiomethyl AAP (SMe-AAP-Ac, Schemes S1−S3, Figure 2A). Gelation is conducted between two glass slides separated by 25 $\mu$m-thick Kapton spacers to set the thickness of the sheets. The gels are cut into discs and, following equilibration in the dark in water overnight, imaged under an optical microscope on a variable-temperature stage to measure the areal swelling ratio, which is calculated as the ratio of the area of the swollen gel to the area of the gel equilibrated at 37 °C, at which point the gels had reached a plateau in the swelling ratio. The gels are assumed to swell isotopically in all directions; thus, the areal swelling ratio is directly translatable to both the linear and volumetric swelling ratios. The swelling change, which is defined as the percent change of the area of the disc upon *trans* to *cis* isomerization, is given by eq 1, where $SR_{405}$ and $SR_{530}$ are the areal swelling ratios at the PSS under 405 and 530 nm light, respectively.

$$\text{swelling change} = \frac{SR_{405} - SR_{530}}{SR_{530}} \times 100\% \quad (1)$$

As seen in Figure 2B,C, the gels demonstrate modest swelling in response to 405 nm irradiation when in water, which we attribute to the higher polarity of the *cis* isomer and is consistent with previous reports on azobenzene-containing gels.[28,29] When the disc is moved to a solution of 8.8 mM $\beta$-CD, and the experiment repeated, a much more substantial


https://doi.org/10.1021/acsapm.4c00917
ACS Appl. Polym. Mater. XXXX, XXX, XXX−XXX

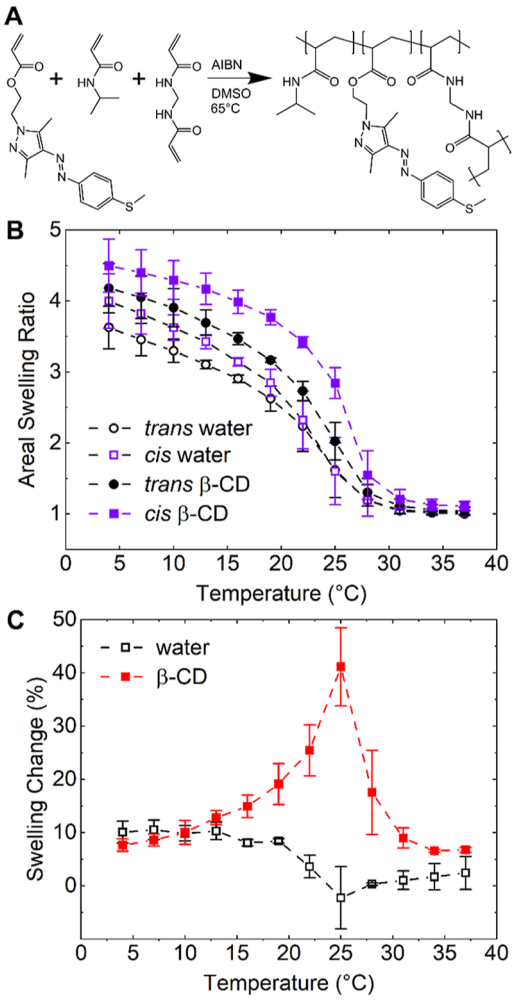


**Figure 2.** (A) Synthetic scheme for free-radical polymerization of SMe-AAP hydrogels. (B) Equilibrium areal swelling ratio versus temperature of SMe-AAP hydrogels in pure water (open symbols) and in 8.8 mM $\beta$-CD solution (filled symbols) in the 530 nm-irradiated, *trans*-rich configuration (black) and in the 405 nm-irradiated, *cis*-rich configuration (purple). (C) Swelling change as a function of temperature in water (black line) and in 8.8 mM $\beta$-CD solution (red line). Error bars represent standard deviations over 3 samples.

response is observed, with a change of up to ≈40% in area upon irradiation at 25 °C. In all cases, the gels exhibit lower critical solution temperature behavior that is characteristic of PNIPAM. Importantly, the deswelling transition is shifted to slightly higher temperatures in the $\beta$-CD solution when the gels are exposed to 405 nm light. The light-triggered swelling response of the SMe-AAP gels is opposite to that of our previously reported host−guest hydrogels, where, upon *trans*−*cis* isomerization, the azobenzene decomplexes from the CD, resulting in a more hydrophobic network and subsequent deswelling.[29] From these results, we hypothesize that the SMe-AAP binds more strongly to the CD in the *cis* configuration than in the *trans* configuration, resulting in a more hydrophilic network in the *cis*-rich state, which drives higher swelling ratios.

To investigate the binding behavior of the SMe-AAP with $\beta$-CD, a linear, water-soluble copolymer containing *N*,*N*-dimethylacrylamide (DMAM) and SMe-AAP-Ac was synthesized (Scheme S4 and Figure S1) and isothermal titration calorimetry (ITC) was conducted to determine the binding constants in the *trans* and the *cis* configurations. DMAM was chosen because a PNIPAM copolymer with equivalent AAP loading was not water-soluble at room temperature. ITC curves fitted to a 1:1 independent binding model are shown in Figure S4. The ITC confirms the somewhat tighter binding of the cis isomer to the $\beta$-CD, with a binding constant of 240 $M^{-1}$ in the *trans* configuration and 450 $M^{-1}$ in the *cis* configuration. We additionally conducted NMR titration as an alternative method to measure the association constants and found good agreement with the ITC data; however, poorer fit quality resulted in significantly larger errors (Figure S5). Generally, substitution of the phenyl ring has a significant impact on the supramolecular complexation of AAPs with $\beta$-CD; however, to our knowledge, no other AAPs have been reported to show stronger binding affinity for the *cis* isomer over the *trans* isomer, leading us to infer that the methyl thioether substituent is responsible for the binding behavior observed here. For example, AAP derivatives with methyl, methoxy, isopropyl, and isopropoxy, and *tert*-butyl groups installed in the para position, as well as the unsubstituted version, have been shown to bind to $\beta$-CD more strongly in the *trans* isomer by factors of approximately 2−9.[36,38]

The host−guest complex was further investigated via nuclear Overhauser effect spectroscopy (NOESY), a 2D NMR experiment that probes cross-relaxation between nuclei that are close in space. To enhance water solubility of the SMe-AAP for the NOESY experiment, a pyridinium salt derivative (SMe-AAP-Py) was synthesized (Scheme S5). We note that a similar strategy was used to conduct NOESY on tetra-*ortho*-methoxy azobenzene.[37] Selected regions of NOESY spectra for dark adapted and *cis*-rich SMe-AAP-Py are shown in Figure 2A,B, respectively. Cross peaks between AAP protons and CD protons in the NOESY spectra indicate that those protons are close in space and thus binding is occurring. Specifically, in the *trans* configuration, cross peaks are seen between the interior protons near the wide rim of the CD ($H_3$) and the methyl protons on the pyrazole ring of the AAP ($H_b$ and $H_c$). Additionally, a weak cross peak is observed between the narrow rim protons of the CD ($H_6$) and the methyl thioether protons of the AAP ($H_a$). In the *cis* configuration, cross peaks are still present between $H_3$ and $H_b$ and $H_c$ ($H_b$ is shifted out of the range of chemical shifts shown in the spectrum); however, the thiomethyl protons $H_a$ now display a strong cross peak with the interior protons near the narrow end of the CD ($H_5$), indicating that the CD now sits further away from the pyrazole end of the AAP. In both isomers, strong peaks are observed between the aromatic protons of the AAP and both interior $H_3$ and $H_5$ of the CD (Figure S6). Importantly, no cross peaks were observed between the CD and any of the protons on the chain linking the AAP to the pyridinium ring, which is consistent with previous work that suggests that the CD cannot pass entirely over the dimethylpyrazole group due to steric bulk.[42] We hypothesize that the bulkiness of both the thiomethyl group and the dimethylpyrazole group is unfavorable to binding, as suggested by the lower binding constants in both isomers compared to similar AAPs. However, in the *cis* configuration, we hypothesize that the rotation of the pyrazole ring out of plane allows for the CD to better accommodate the bulky thiomethyl group, as evidenced by the shift away from the dimethylpyrazole ring, resulting in more favorable binding. We note that a more in-depth study is necessary to elucidate a detailed binding mechanism.


https://doi.org/10.1021/acsapm.4c00917
ACS Appl. Polym. Mater. XXXX, XXX, XXX−XXX

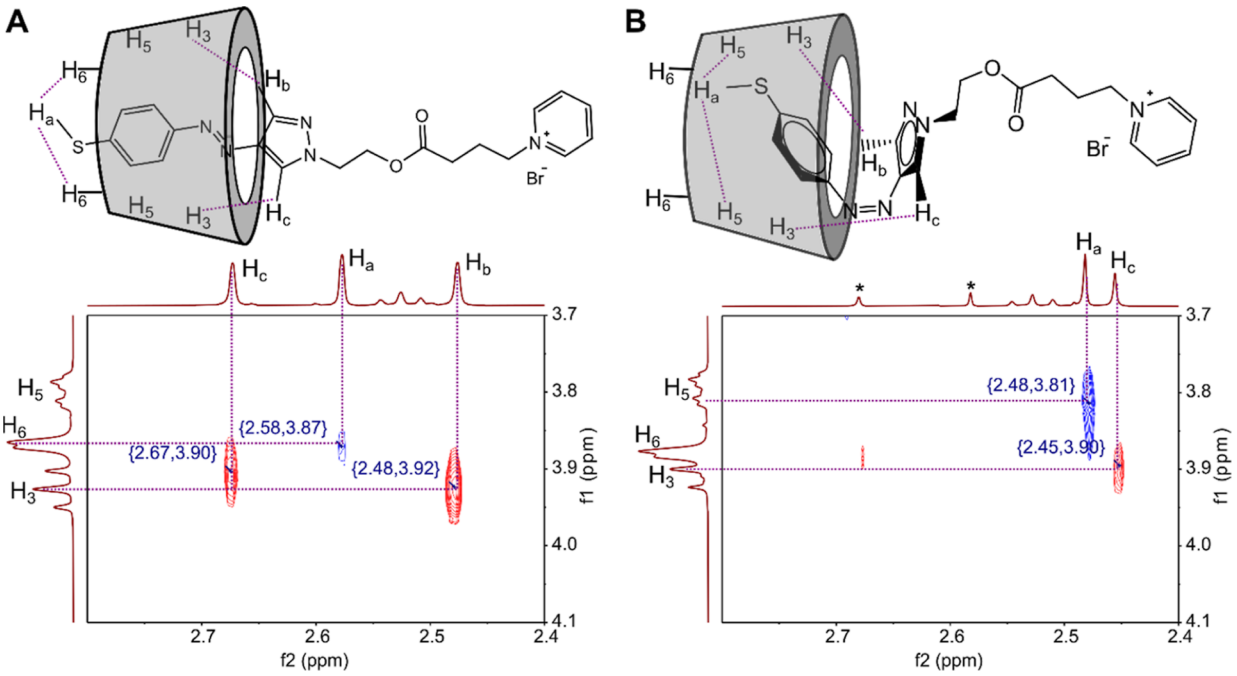


**Figure 3.** Schematics and selected region of 2D-NOESY spectra of SMe-AAP-Py and $\beta$-CD for (A) dark adapted, *trans* configuration and (B) 405 nm-irradiated, *cis*-rich configuration. Purple dashed lines indicate through-space correlations of nearby protons. Asterisks denote residual *trans* peaks in the *cis* spectrum due to incomplete switching.

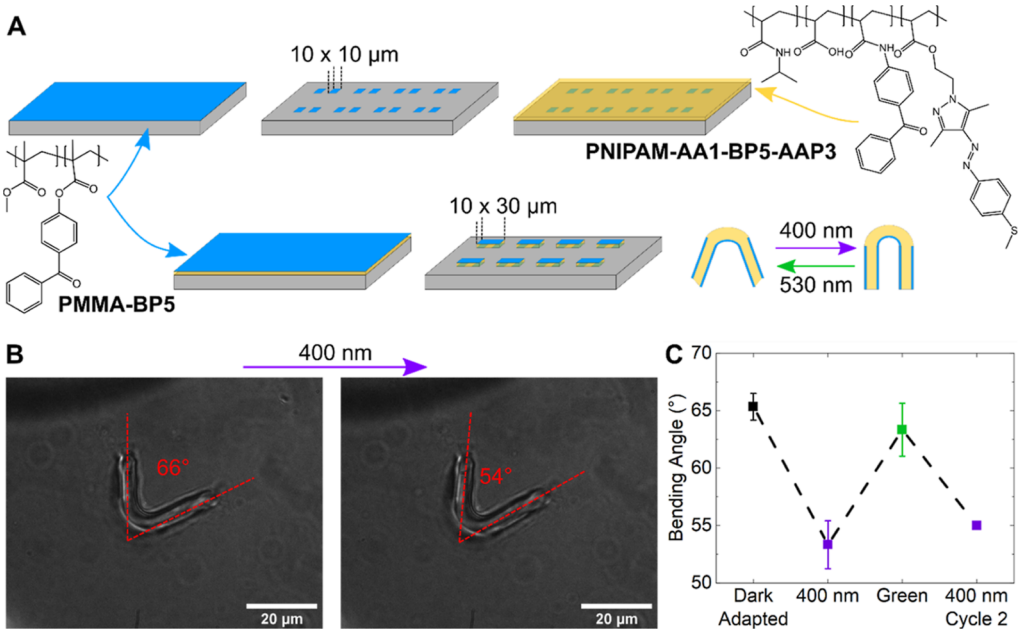


**Figure 4.** (A) Fabrication procedure of light-responsive trilayer microhinges using maskless lithography. (B) Optical micrographs showing the change in bending angle of the hinges upon light irradiation (400 nm, 25 mW/cm$^2$). (C) Bending angle of the hinges plotted against the irradiation cycle.

Next, we demonstrate that the reversible host−guest complexation between the AAP and $\beta$-CD can be used to create microactuators using a trilayer fabrication scheme. First, two linear polymers containing 5 mol % of photo-cross-linkable benzophenone derivative as a comonomer were synthesized: a poly(methyl methacrylate) (PMMA-BP5) and a poly(*N*-isopropylacrylamide), which also contains SMe-AAP-Ac at 3 mol % to impart light responsiveness and acrylic acid at 1 mol % to increase swelling (PNIPAM-AA1-BP5-AAP3) (synthetic details are given in Schemes S8 and S9). The polymer structures, as well as the trilayer fabrication scheme, are shown in Figure 3A. In short, a thin (∼100 nm) film of PMMA-BP5 was spin-coated onto a poly(vinyl alcohol) release layer on a silicon substrate, and pairs of 10 $\mu$m by 10 $\mu$m squares with a gap of 10 $\mu$m were fabricated using maskless lithography. Following development, a thick (∼1 $\mu$m) layer of PNIPAM-AA1-BP5-AAP3 and another thin (∼100 $\mu$m) film of PMMA-BP5 were spin-coated, and rectangles connecting the pairs of squares were fabricated and developed. Upon development and release into dilute phosphate-buffered saline


https://doi.org/10.1021/acsapm.4c00917
ACS Appl. Polym. Mater. XXXX, XXX, XXX−XXX

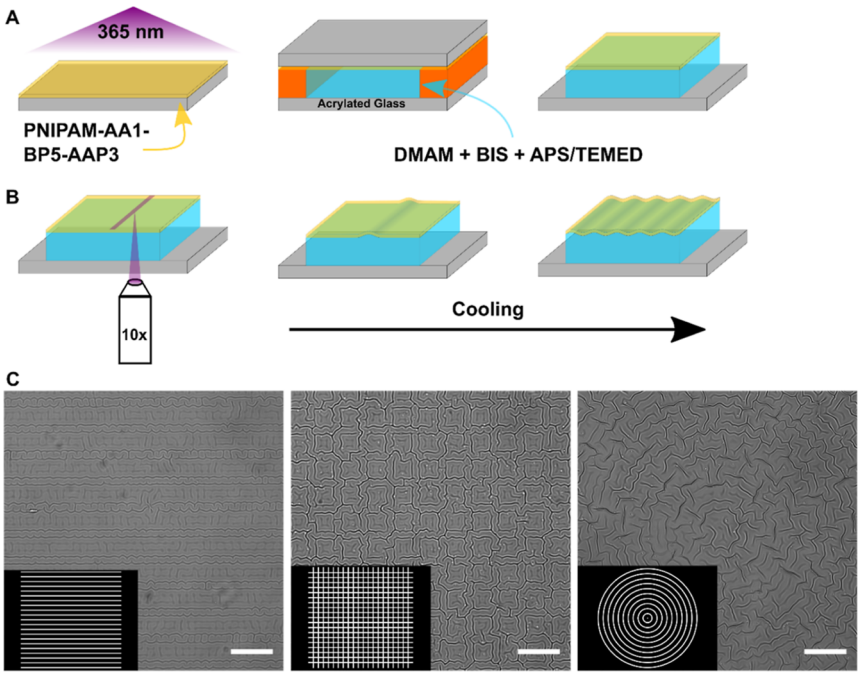


**Figure 5.** (A) Fabrication procedure of wrinkling bilayers using a photo-cross-linkable and light-responsive thin film on a passive, soft layer, which is attached to a glass substrate. (B) Photopatterning scheme of wrinkling bilayers wherein 400 nm light (25 mW/cm$^2$) is projected off a digital micromirror array and through a 10x microscope objective focused onto the bilayer. (C) Optical micrographs of bilayer films after being cooled to room temperature to induce wrinkling. Insets show the pattern of light projected onto the bilayer. Scale bars represent 80 $\mu$m.

with 8.8 mM $\beta$-CD, the particles bend into a "hinge" shape, since the PMMA layers prevent in-plane expansion of the PNIPAM layer. This strategy has been previously employed by our group to fabricate a self-folding origami.[43]

The hinges are imaged under an inverted microscope equipped with a 100x objective lens and digital micromirror array to project light onto the sample, as well as a 400 nm LED and a white light source that passes through a 520−540 nm filter cube to produce green light (the equipment setup is described in detail elsewhere).[44] Figure 4B illustrates the bending behavior of the hinge in response to illumination. The dark equilibrated hinges bend to an internal angle of 66°, and upon irradiation with 400 nm light (25 mW/cm$^2$), the bending angle decreases to 54°. Irradiation with green light reverts the hinge nearly back to the original bending angle (Figure 4C). Importantly, since the PNIPAM layers are thin, these responses occur in only a few seconds, since the process is limited by poroelastic diffusion of water through the polymer network.[45] Videos of the actuation behavior in response to 400 nm light and green light are shown in Videos S1 and S2, respectively. Although further optimization of geometry and material parameters is necessary to improve the magnitude of the light response, this approach represents a proof-of-concept design for hydrogel-based photoactuators on the micron scale.

Finally, the AAP-containing hydrogel was used in a bilayer construction to generate photochemically patterned surface wrinkles by leveraging a swelling-induced mechanical instability. When a thin, hard layer is fixed to a thick, soft layer and the bilayer is subjected to a compressive stress that exceeds a critical value, the structure will undergo a mechanical instability and form periodic wrinkles.[46] The critical strain for wrinkle formation $\varepsilon_c$ and the wavelength $\lambda$ of the resulting wrinkles are given by eqs 2 and 3, respectively, where $\bar{E}_h$ and $\bar{E}_s$ are the plane strain moduli of the hard and soft layer, respectively, and $t_h$ is the thickness of the hard layer.[47]

$$\varepsilon_c = \frac{1}{4}\left(\frac{3\bar{E}_s}{\bar{E}_h}\right)^{2/3} \quad (2)$$

$$\lambda = 2\pi t_h\left(\frac{\bar{E}_h}{3\bar{E}_s}\right)^{1/3} \quad (3)$$

We use the AAP-containing, photo-cross-linkable polymer PNIPAM-AA1-BP5-AAP3 as the thin, hard layer by first drop-casting the polymer onto a glass slide and uniformly curing the film with 365 nm light. The slide and film are then made into a cell with a second glass slide, which has been treated with the adhesion promoter 3-(trimethoxysilyl)propyl methacrylate to form covalent bonds between the hydrogel and the glass substrate, and 125 $\mu$m-thick Kapton spacers. A solution of DMAM, BIS, ammonium persulfate, and tetramethylethylenediamine is then infiltrated into the cell and allowed to gel to form the soft layer. This process is illustrated in Figure 5A and described in greater detail in the Supporting Information. Upon infiltration, the DMAM pregel solution swells into the hard film layer and forms an interpenetrating network structure that facilitates adhesion between the layers; however, this swelling is not extensive enough to delaminate the film from the slide it was cast on. We found that when the PNIPAM polymer film instead contained 5 mol % acrylic acid, the high degree of swelling following infiltration caused complete delamination of the film from the glass. The bilayer samples are allowed to gel and are then immersed in 45 °C deionized water for ≈3 days to fully delaminate from the glass substrate. Warm water is used to prevent the bilayer from wrinkling before light patterning can be conducted.

We estimate that the hard PNIPAM layer has a plane strain modulus of ≈400 kPa,[48] and the thickness of this film is approximately 1−2 $\mu$m. The monomer and cross-linker concentration of the DMAM layer was tailored to target a


https://doi.org/10.1021/acsapm.4c00917
ACS Appl. Polym. Mater. XXXX, XXX, XXX−XXX

plane strain modulus of ≈90 kPa.[49,50] These moduli result in a calculated critical strain of approximately 19% from eq 2, which would enable a transition from flat to wrinkled during cooling of the bilayer due to the swelling of the thermoresponsive hard layer to a linear strain of around 30% at room temperature. The calculated wavelength of the resulting wrinkles from eq 3 is 7−14 μm. When the bilayers are released and allowed to swell in room temperature water in the absence of light, a mixture of herringbone and disordered wrinkles with a wavelength of ≈13 μm develops (Figure S7). Both wrinkle morphologies are possible under biaxial compression.[51]

We then employ the inverted microscope and digital micromirror array described above to project patterned 400 nm light onto the bilayers before cooling. Because the *cis*-rich gels display a shift of the deswelling transition to slightly higher temperatures, cooling of the bilayer will cause the illuminated regions to cross the critical threshold for wrinkling before the rest of the sample, thus creating patterned wrinkles. These initial wrinkles then direct the pattern of the nonpatterned regions when they cross the wrinkling threshold (Figure 5B). Several patterns are used, as indicated in Figure 5C, where the inset shows the projected 400 nm light pattern, and the image shows the wrinkled bilayer after cooling to room temperature. Images of the entire field of view are given in Figure S8. We found that the pattern from the illuminated regions was able to direct pattern formation in the nonilluminated regions within a range of ≈20−30 μm in each direction. Therefore, patterns were designed with a line-to-line distance of 40 μm. When a large spacing was used, the pattern failed to fully propagate between illuminated regions (Figure S9). Importantly, the wrinkles could be erased by immersion in warm water again, allowing the same sample to be reused multiple times for a variety of patterns. Videos of cooling and wrinkle formation as well as heating and wrinkle erasure are given in Videos S3−S5. Although photochemically patterned surface wrinkles have been demonstrated previously using mechanisms such as anthracene dimerization,[52,53] and azobenzene isomerization[54] in polymeric systems, this approach represents a straightforward method for photochemical patterning of surface wrinkles in a hydrogel, which has potential for biological applications such as dynamic cell culture substrates.

## ■ CONCLUSIONS

In conclusion, we have developed light-responsive supramolecular hydrogels that operate entirely under visible light by using the photoreversible host−guest complexation between thiomethyl-substituted AAP and β-CD. We found that this AAP exhibits stronger binding to the β-CD in the *cis* configuration than in the *trans* configuration, a result opposite to previously reported systems. This binding behavior results in swelling of the hydrogel under *trans* to *cis* isomerization using purple light that is rapid and reversible. We then employ the hydrogels in a trilayer construction to demonstrate light-induced bending as well as in a bilayer construction to demonstrate patterned surface wrinkles using light. Given the high degree of biocompatibility afforded by hydrogels and the absence of cytotoxic UV light, these design concepts are anticipated to assist in future creation of advanced, dynamic materials that can be interfaced with cells and biological tissues.

## ■ ASSOCIATED CONTENT

### Supporting Information

The Supporting Information is available free of charge at https://pubs.acs.org/doi/10.1021/acsapm.4c00917.

Materials, equipment, detailed experimental methods, photoswitching data of the AAP monomer, ITC, NMR titration study, full NOESY spectra of AAP/β-CD complexes, and optical micrographs of the bilayer film of PNIPAM and PDMAM and of wrinkles patterned with 10 μm-thick horizontal lines with a line-to-line spacing of 110 μm and full field of view optical micrographs of wrinkled bilayers (PDF)

400 nm exposure of the trilayer microhinge (MP4)

Green-light exposure of the trilayer microhinge (MP4)

Straight-line wrinkle formation during cooling (MP4)

Concentric-ring wrinkle formation during cooling (MP4)

Heating and erasure of straight-line wrinkles (MP4)

## ■ AUTHOR INFORMATION


### Corresponding Authors

**Kesete Ghebreyessus** − *Department of Chemistry and Biochemistry, Hampton University, Hampton, Virginia 23668, United States;* orcid.org/0000-0003-4273-7556; Email: Kesete.Ghebreyessus@hamptonu.edu

**Ryan C. Hayward** − *Department of Chemical and Biological Engineering, University of Colorado Boulder, Boulder, Colorado 80303, United States; Materials Science and Engineering Program, University of Colorado Boulder, Boulder, Colorado 80303, United States;* orcid.org/0000-0001-6483-2234; Email: ryan.hayward@colorado.edu

### Authors

**Joseph C. Roback** − *Department of Chemical and Biological Engineering, University of Colorado Boulder, Boulder, Colorado 80303, United States*

**Montana B. Minnis** − *Department of Chemical and Biological Engineering, University of Colorado Boulder, Boulder, Colorado 80303, United States*

Complete contact information is available at: https://pubs.acs.org/10.1021/acsapm.4c00917


### Author Contributions

The manuscript was written through contributions of all authors. All authors have given approval to the final version of the manuscript.

### Notes

The authors declare no competing financial interest.

## ■ ACKNOWLEDGMENTS

This work was supported by the Brandeis MRSEC through grant DMR-2011846 and by the National Science Foundation Hampton-Brandeis Partnership for Research and Education in Materials (PREM) through grant 1827820. M.B.M. acknowledges support from the National Defense Science and Engineering (NDSEG) Fellowship Program.

## ■ REFERENCES

(1) Jeon, S.-J.; Hauser, A. W.; Hayward, R. C. Shape-Morphing Materials from Stimuli-Responsive Hydrogel Hybrids. *Acc. Chem. Res.* **2017**, *50* (2), 161−169.

(2) Kim, J.; Hanna, J. A.; Byun, M.; Santangelo, C. D.; Hayward, R. C. Designing Responsive Buckled Surfaces by Halftone Gel Lithography. *Science* **2012**, *335* (6073), 1201−1205.
(3) Ionov, L. Hydrogel-Based Actuators: Possibilities and Limitations. *Mater. Today* **2014**, *17* (10), 494−503.
(4) Li, C.; Kazem-Rostami, M.; Seale, J. S. W.; Zhou, S.; Stupp, S. I. Macroscopic Actuation of Bisazo Hydrogels Driven by Molecular Photoisomerization. *Chem. Mater.* **2023**, *35* (10), 3923−3930.
(5) Li, C.; Lau, G. C.; Yuan, H.; Aggarwal, A.; Dominguez, V. L.; Liu, S.; Sai, H.; Palmer, L. C.; Sather, N. A.; Pearson, T. J.; Freedman, D. E.; Amiri, P. K.; de la Cruz, M. O.; Stupp, S. I. Fast and Programmable Locomotion of Hydrogel-Metal Hybrids under Light and Magnetic Fields. *Sci. Robot.* **2020**, *5* (49), No. eabb9822.
(6) Zhao, Y.; Xuan, C.; Qian, X.; Alsaid, Y.; Hua, M.; Jin, L.; He, X. Soft Phototactic Swimmer Based on Self-Sustained Hydrogel Oscillator. *Sci. Robot.* **2019**, *4* (33), No. eaax7112.
(7) Kloxin, A. M.; Kasko, A. M.; Salinas, C. N.; Anseth, K. S. Photodegradable Hydrogels for Dynamic Tuning of Physical and Chemical Properties. *Science* **2009**, *324* (5923), 59−63.
(8) Käpylä, E.; Delgado, S. M.; Kasko, A. M. Shape-Changing Photodegradable Hydrogels for Dynamic 3D Cell Culture. *ACS Appl. Mater. Interfaces* **2016**, *8* (28), 17885−17893.
(9) Hoffman, A. S. Hydrogels for Biomedical Applications. *Adv. Drug Delivery Rev.* **2012**, *64*, 18−23.
(10) Koetting, M. C.; Peters, J. T.; Steichen, S. D.; Peppas, N. A. Stimulus-Responsive Hydrogels: Theory, Modern Advances, and Applications. *Mater. Sci. Eng.: R: Rep.* **2015**, *93*, 1−49.
(11) Stowers, R. S.; Allen, S. C.; Suggs, L. J. Dynamic Phototuning of 3D Hydrogel Stiffness. *Proc. Natl. Acad. Sci. U.S.A.* **2015**, *112* (7), 1953−1958.
(12) Hauser, A. W.; Evans, A. A.; Na, J.-H.; Hayward, R. C. Photothermally Reprogrammable Buckling of Nanocomposite Gel Sheets. *Angew. Chem., Int. Ed.* **2015**, *54* (18), 5434−5437.
(13) Shi, Q.; Xia, H.; Li, P.; Wang, Y.-S.; Wang, L.; Li, S.-X.; Wang, G.; Lv, C.; Niu, L.-G.; Sun, H.-B. Photothermal Surface Plasmon Resonance and Interband Transition-Enhanced Nanocomposite Hydrogel Actuators with Hand-Like Dynamic Manipulation. *Adv. Opt. Mater.* **2017**, *5* (22), 1700442.
(14) Zhu, Z.; Senses, E.; Akcora, P.; Sukhishvili, S. A. Programmable Light-Controlled Shape Changes in Layered Polymer Nanocomposites. *ACS Nano* **2012**, *6* (4), 3152−3162.
(15) Kim, H.; Kang, J.-H.; Zhou, Y.; Kuenstler, A. S.; Kim, Y.; Chen, C.; Emrick, T.; Hayward, R. C. Light-Driven Shape Morphing, Assembly, and Motion of Nanocomposite Gel Surfers. *Adv. Mater.* **2019**, *31* (27), 1900932.
(16) Kim, D.; Lee, H. S.; Yoon, J. Highly Bendable Bilayer-Type Photo-Actuators Comprising of Reduced Graphene Oxide Dispersed in Hydrogels. *Sci. Rep.* **2016**, *6* (1), 20921.
(17) Kuenstler, A. S.; Hayward, R. C. Light-Induced Shape Morphing of Thin Films. *Curr. Opin. Colloid Interface Sci.* **2019**, *40*, 70−86.
(18) Satoh, T.; Sumaru, K.; Takagi, T.; Kanamori, T. Fast-Reversible Light-Driven Hydrogels Consisting of Spirobenzopyran-Functionalized Poly(N-Isopropylacrylamide). *Soft Matter* **2011**, *7* (18), 8030−8034.
(19) Li, C.; Iscen, A.; Palmer, L. C.; Schatz, G. C.; Stupp, S. I. Light-Driven Expansion of Spiropyran Hydrogels. *J. Am. Chem. Soc.* **2020**, *142* (18), 8447−8453.
(20) Kuksenok, O.; Balazs, A. C. Modeling the Photoinduced Reconfiguration and Directed Motion of Polymer Gels. *Adv. Funct. Mater.* **2013**, *23* (36), 4601−4610.
(21) Ziółkowski, B.; Florea, L.; Theobald, J.; Benito-Lopez, F.; Diamond, D. Self-Protonating Spiropyran- Co -NIPAM- Co -Acrylic Acid Hydrogel Photoactuators. *Soft Matter* **2013**, *9* (36), 8754−8760.
(22) Kortekaas, L.; Browne, W. R. The Evolution of Spiropyran: Fundamentals and Progress of an Extraordinarily Versatile Photochrome. *Chem. Soc. Rev.* **2019**, *48* (12), 3406−3424.
(23) Chen, J.; Huang, J.; Zhang, H.; Hu, Y. A Photoresponsive Hydrogel with Enhanced Photoefficiency and the Decoupled Process of Light Activation and Shape Changing for Precise Geometric Control. *ACS Appl. Mater. Interfaces* **2020**, *12* (34), 38647−38654.
(24) Xiang, S.-L.; Su, Y.-X.; Yin, H.; Li, C.; Zhu, M.-Q. Visible-Light-Driven Isotropic Hydrogels as Anisotropic Underwater Actuators. *Nano Energy* **2021**, *85*, 105965.
(25) Jiang, Z.; Tan, M. L.; Taheri, M.; Yan, Q.; Tsuzuki, T.; Gardiner, M. G.; Diggle, B.; Connal, L. A. Strong, Self-Healable, and Recyclable Visible-Light-Responsive Hydrogel Actuators. *Angew. Chem.* **2020**, *132* (18), 7115−7122.
(26) Amir, F.; Li, X.; Gruschka, M. C.; Colley, N. D.; Li, L.; Li, R.; Linder, H. R.; Sell, S. A.; Barnes, J. C. Dynamic, Multimodal Hydrogel Actuators Using Porphyrin-Based Visible Light Photoredox Catalysis in a Thermoresponsive Polymer Network. *Chem. Sci.* **2020**, *11* (40), 10910−10920.
(27) Barrett, C. J.; Mamiya, J.; Yager, K. G.; Ikeda, T. Photo-Mechanical Effects in Azobenzene-Containing Soft Materials. *Soft Matter* **2007**, *3* (10), 1249−1261.
(28) Matsubara, K.; Watanabe, M.; Takeoka, Y. A Thermally Adjustable Multicolor Photochromic Hydrogel. *Angew. Chem., Int. Ed.* **2007**, *46* (10), 1688−1692.
(29) Kuenstler, A. S.; Lahikainen, M.; Zhou, H.; Xu, W.; Priimagi, A.; Hayward, R. C. Reconfiguring Gaussian Curvature of Hydrogel Sheets with Photoswitchable Host-Guest Interactions. *ACS Macro Lett.* **2020**, *9* (8), 1172−1177.
(30) Harada, A. Cyclodextrin-Based Molecular Machines. *Acc. Chem. Res.* **2001**, *34* (6), 456−464.
(31) Tomatsu, I.; Hashidzume, A.; Harada, A. Photoresponsive Hydrogel System Using Molecular Recognition of $\alpha$-Cyclodextrin. *Macromolecules* **2005**, *38* (12), 5223−5227.
(32) Zhao, Y.-L.; Stoddart, J. F. Azobenzene-Based Light-Responsive Hydrogel System. *Langmuir* **2009**, *25* (15), 8442−8446.
(33) Rosales, A. M.; Rodell, C. B.; Chen, M. H.; Morrow, M. G.; Anseth, K. S.; Burdick, J. A. Reversible Control of Network Properties in Azobenzene-Containing Hyaluronic Acid-Based Hydrogels. *Bioconjugate Chem.* **2018**, *29* (4), 905−913.
(34) Iwaso, K.; Takashima, Y.; Harada, A. Fast Response Dry-Type Artificial Molecular Muscles with [C2]Daisy Chains. *Nat. Chem.* **2016**, *8* (6), 625−632.
(35) Ma, W.; Fang, H.; Tian, D.; Zheng, L.; Xie, M.; Sun, R. Solvent-Free Stretchable Photo-Responsive Supramolecular Actuator Topologically Cross-Linked by Azobenzene-Cyclodextrin Based Slide-Ring System. *Dyes Pigm.* **2022**, *200*, 110120.
(36) Stricker, L.; Bockmann, M.; Kirse, T.; Doltsinis, N.; Ravoo, B. Arylazopyrazole Photoswitches in Aqueous Solution: Substituent Effects, Photophysical Properties, and Host-Guest Chemistry. *Chemistry* **2018**, *24*, 8639−8647.
(37) Wang, D.; Wagner, M.; Butt, H.-J.; Wu, S. Supramolecular Hydrogels Constructed by Red-Light-Responsive Host-Guest Interactions for Photo-Controlled Protein Release in Deep Tissue. *Soft Matter* **2015**, *11* (38), 7656−7662.
(38) Lamping, S.; Stricker, L.; Ravoo, B. J. Responsive Surface Adhesion Based on Host-Guest Interaction of Polymer Brushes with Cyclodextrins and Arylazopyrazoles. *Polym. Chem.* **2019**, *10* (6), 683−690.
(39) Lee, D. C.; Guye, K. N.; Paranji, R. K.; Lachowski, K.; Pozzo, L. D.; Ginger, D. S.; Pun, S. H. Dual-Stimuli Responsive Single-Chain Polymer Folding via Intrachain Complexation of Tetramethoxyazobenzene and $\beta$-Cyclodextrin. *Langmuir* **2021**, *37* (33), 10126−10134.
(40) Yan, H.; Qiu, Y.; Wang, J.; Jiang, Q.; Wang, H.; Liao, Y.; Xie, X. Wholly Visible-Light-Responsive Host−Guest Supramolecular Gels Based on Methoxy Azobenzene and $\beta$-Cyclodextrin Dimers. *Langmuir* **2020**, *36* (26), 7408−7417.
(41) Bhunia, S.; Dolai, A.; Samanta, S. Robust Bi-Directional Photoswitching of Thiomethyl Substituted Arylazopyrazoles under Visible Light. *Chem. Commun.* **2020**, *56* (70), 10247−10250.
(42) Stricker, L.; Fritz, E.-C.; Peterlechner, M.; Doltsinis, N. L.; Ravoo, B. J. Arylazopyrazoles as Light-Responsive Molecular Switches in Cyclodextrin-Based Supramolecular Systems. *J. Am. Chem. Soc.* **2016**, *138* (13), 4547−4554.


https://doi.org/10.1021/acsapm.4c00917
ACS Appl. Polym. Mater. XXXX, XXX, XXX−XXX

(43) Na, J.-H.; Evans, A. A.; Bae, J.; Chiappelli, M. C.; Santangelo, C. D.; Lang, R. J.; Hull, T. C.; Hayward, R. C. Programming Reversibly Self-Folding Origami with Micropatterned Photo-Cross-linkable Polymer Trilayers. *Adv. Mater.* **2015**, *27* (1), 79−85.
(44) Limberg, D. K.; Kang, J.-H.; Hayward, R. C. Triplet-Triplet Annihilation Photopolymerization for High-Resolution 3D Printing. *J. Am. Chem. Soc.* **2022**, *144* (12), 5226−5232.
(45) Yoon, J.; Cai, S.; Suo, Z.; Hayward, R. C. Poroelastic Swelling Kinetics of Thin Hydrogel Layers: Comparison of Theory and Experiment. *Soft Matter* **2010**, *6* (23), 6004−6012.
(46) Yang, S.; Khare, K.; Lin, P.-C. Harnessing Surface Wrinkle Patterns in Soft Matter. *Adv. Funct. Mater.* **2010**, *20* (16), 2550−2564.
(47) Chen, C.-M.; Yang, S. Wrinkling Instabilities in Polymer Films and Their Applications. *Polym. Int.* **2012**, *61* (7), 1041−1047.
(48) Bae, J.; Ouchi, T.; Hayward, R. C. Measuring the Elastic Modulus of Thin Polymer Sheets by Elastocapillary Bending. *ACS Appl. Mater. Interfaces* **2015**, *7* (27), 14734−14742.
(49) Gundogan, N.; Okay, O.; Oppermann, W. Swelling, Elasticity and Spatial Inhomogeneity of Poly(N,N-Dimethylacrylamide) Hydrogels Formed at Various Polymer Concentrations. *Macromol. Chem. Phys.* **2004**, *205* (6), 814−823.
(50) Ikeda-Fukazawa, T.; Ikeda, N.; Tabata, M.; Hattori, M.; Aizawa, M.; Yunoki, S.; Sekine, Y. Effects of Crosslinker Density on the Polymer Network Structure in Poly-N,N-Dimethylacrylamide Hydrogels. *J. Polym. Sci., Part B: Polym. Phys.* **2013**, *51* (13), 1017−1027.
(51) Lin, P.-C.; Yang, S. Spontaneous Formation of One-Dimensional Ripples in Transit to Highly Ordered Two-Dimensional Herringbone Structures through Sequential and Unequal Biaxial Mechanical Stretching. *Appl. Phys. Lett.* **2007**, *90* (24), 241903.
(52) Hou, H.; Yin, J.; Jiang, X. Smart Patterned Surface with Dynamic Wrinkles. *Acc. Chem. Res.* **2019**, *52* (4), 1025−1035.
(53) Chen, S.; Hu, K.; Yan, S.; Ma, T.; Deng, X.; Zhang, W.; Yin, J.; Jiang, X. Dynamic Metal Patterns of Wrinkles Based on Photosensitive Layers. *Sci. Bull.* **2022**, *67*, 2186−2195.
(54) Zong, C.; Zhao, Y.; Ji, H.; Han, X.; Xie, J.; Wang, J.; Cao, Y.; Jiang, S.; Lu, C. Tuning and Erasing Surface Wrinkles by Reversible Visible-Light-Induced Photoisomerization. *Angew. Chem., Int. Ed.* **2016**, *55* (12), 3931−3935.


https://doi.org/10.1021/acsapm.4c00917
ACS Appl. Polym. Mater. XXXX, XXX, XXX−XXX